

Soil Salinity Mapping by Multiscale Remote Sensing in Mesopotamia, Iraq

Weicheng Wu, Waleed M. Al-Shafie, Ahmad S. Mhaimed, Feras Ziadat, Vinay Nangia, and William Bill Payne

Abstract—Soil salinity has become one of the major problems affecting crop production and food security in Mesopotamia, Iraq. There is a pressing need to quantify and map the spatial extent and distribution of salinity in the country in order to provide relevant references for the central and local governments to plan sustainable land use and agricultural development. The aim of this study was to conduct such quantification and mapping in Mesopotamia using an integrated, multiscale modeling approach that relies on remote sensing. A multiyear, multiresolution, and multisensor dataset composed of mainly Landsat ETM+ and MODIS data of the period 2009–2012 was used. Results show that the local-scale salinity models developed from pilot sites with vegetated and nonvegetated areas can reliably predict salinity. Salinity maps produced by these models have a high accuracy of about 82.5–83.3% against the ground measurements. Regional salinity models developed using integrated samples from all pilot sites could predict soil salinity with an accuracy of 80% based on comparison to regional measurements along two transects. It is hence concluded that the multiscale models are reasonably reliable for assessment of soil salinity at local and regional scales. The methodology proposed in this paper can minimize problems induced by crop rotation, fallowing, and soil moisture content, and has clear advantages over other mapping approaches. Further testing is needed while extending the mapping approaches and models to other salinity-affected environments.

Index Terms—Multiscale remote sensing, multiyear maxima, new processing algorithm, salinity models, soil salinity.

I. INTRODUCTION

APPROXIMATELY, 60% of the cultivated land in the Mesopotamian plain in Iraq is seriously affected by salinity [1]; 20–30% has been abandoned in the past 4000 years [1], [2]. Because of soil salinity, yield of crops, especially, wheat of nonabandoned has declined by 20–50% by 1950s [2]. But

Manuscript received November 14, 2013; revised July 09, 2014; accepted September 18, 2014. This work was supported in part by the Australian Center for International Agricultural Research (ACIAR) and in part by the Italian Government. (Corresponding author: Weicheng Wu.)

W. Wu was with the International Center for Agricultural Research in the Dry Areas (ICARDA), 11195 Amman, Jordan. He is now an independent scientist in Choisy-Le-Roi 94600, France (e-mail: wuw123@gmail.com).

W. M. Al-Shafie is with the GIS Division, Ministry of Agriculture (MoA), 10001 Baghdad, Iraq.

A. S. Mhaimed is with the College of Agriculture, Baghdad University, 00964 Baghdad, Iraq.

F. Ziadat and V. Nangia are with the Integrated Water and Land Management Program (IWLM), ICARDA, 11195 Amman, Jordan.

W. B. Payne was with ICARDA, 11195 Amman, Jordan. He is now with the College of Agriculture, Biotechnology and Natural Resources (CABNR), University of Nevada, Reno, NV 89557-0221, USA.

Color versions of one or more of the figures in this paper are available online at <http://ieeexplore.ieee.org>.

Digital Object Identifier 10.1109/JSTARS.2014.2360411

the severity and distribution of soil salinity varies with space and time [2]–[4]. In order to prioritize any remediation effort and better plan for agricultural improvements and food security, it is of prime importance for Iraqi central and local governments to understand the distribution and severity of salinity in Mesopotamia.

Soil salinity is a common form of land degradation in irrigated areas located in dryland environments [5]–[8]. The physical appearance of salinity is strongly influenced by soil properties (e.g., moisture, texture, mineral composition, and surface roughness) as well as type of vegetation cover (e.g., halophyte and nonhalophyte, salt-tolerant and nonsalt-tolerant) [5]–[8]. Remote sensing has been widely applied for mapping and assessment of soil salinity in recent decades using vegetation indices (VIs) and combined spectral response index (COSRI) [9]–[16], best band combination [17], [18], maximum likelihood and fuzzy logic-based classifications [19]–[23], principal component analysis (PCA), surface feature unmixing, and data fusion [6], [7], [24]. Predictive models have been developed for soil salinity using different regression analysis, artificial neural network (ANN), and Kriging/CoKriging techniques [9]–[16], [18], [24]–[26]. Very recently, along with vegetation indices and reflectance of certain spectral bands, evapotranspiration (ET) and land surface temperature (LST) have been used to predict salinity in salt-affected areas [16], [27]–[29].

While these and other studies demonstrate the feasibility, advantages, and potential of remote sensing to assess soil salinity, there remain certain challenges. First, although in strongly salinized areas, salt tends to concentrate on terrain surfaces and can be easily detected by conventional remote sensing tools; however, for low-to-moderate salinity (salt <10–15%), spectral confusions with other different surface features may arise leading to identification failure (either overestimation or underestimation) [6], [7]; especially, when salt concentrates in subsoil, optical remote sensing is restricted [8]. Second, soil moisture, halophyte vegetation, and salt-tolerant crops such as barley, cotton, and alfalfa can modify the overall spectral response pattern of salt-affected soils, especially in the green and red bands [6], [7], [30]. Third, lands in the states of fallow, noncrop interval in-between rotations, and crop rotations tend to be interpreted as salinized areas if only soil bareness or vegetation greenness of a single image is investigated. To avoid these problems, some authors have suggested: 1) to use images acquired at the end of dry or hot season or of multiple cropping periods [7], [8], 2) to conduct regression analysis against VIs [9]–[16] and geophysical measurement [8] in combination with

84 soil sampling and analysis. These are, no doubt, useful sugges-
 85 tions to minimize the mentioned problems and accomplish a
 86 better mapping work. However, most of the available studies
 87 have employed single or multirate single images to assess salin-
 88 ity at local scale, and their approaches are not fully repeatable
 89 or extendable for regional-scale assessment due to spatial vari-
 90 ability and diversity in climate conditions, soil properties, and
 91 land use/management. It is, therefore, essential to develop new
 92 processing methods and approaches technically operational for
 93 regional-scale salinity mapping.

94 The main objectives of this study are, hence, to develop an
 95 integrated methodology operational for regional salinity quan-
 96 tification and assessment based on the available approaches
 97 considering the above-mentioned problematic issues, to pro-
 98 vide relevant multiscale salinity maps for Iraqi governments,
 99 and finally, to lay a foundation for the successive regional-scale
 100 tracking of salinity change trends in space and time that may
 101 provide spatial reference for the governments to understand
 102 the impacts of land management on salinization processes in
 103 Mesopotamia.

104 As well as for salinity assessment, remote sensing technol-
 105 ogy has also been widely applied in other dryland research.
 106 Some scientists have utilized annual maximum (peak) VIs
 107 such as Normalized Difference Vegetation Index (NDVI) [31]
 108 to compose cloud-free NDVI [32]–[35] for assessing dryland
 109 biomass [33]–[35] and land degradation [35]–[37] in the past
 110 decades. Others have used multiyear maximum (peak) and min-
 111 imum (trough) NDVI and LST to derive vegetation condition
 112 index (VCI) and temperature condition index (TCI) for mon-
 113 itoring droughts [38]–[40]. Clearly, annual maximum VI, if
 114 applied to salinity assessment, can resolve the problems related
 115 to cloud-cover and crop rotation (crops cultivated either in
 116 spring or summer) but cannot remove that resulted from fal-
 117 low state which may last a couple of years. However, multiyear
 118 maximum, if the observation period spans 3–4 years, can min-
 119 imize (if cannot completely resolve) these problems. LST is
 120 associated with soil moisture and water content [41]–[44], and
 121 high LST is related to low moisture [44]. Thus, multiyear max-
 122 imal LST is a promising indicator to minimize the problem
 123 related to soil moisture.

124 Additionally, remote sensing-based multiscale modeling has
 125 gained a momentum in regional, continental or even global
 126 scale application [34], [45], [46] to extend plot measurements to
 127 local-scale (e.g., pilot site or watershed), and then to regional-
 128 or continental-scale [34], [46]. As Farifteh *et al.* [8] and Wu
 129 *et al.* [34] explained, such multiscale modeling is in fact an
 130 upscaling procedure to extend models developed from local
 131 studies to regional-scale assessment considering the spatial
 132 variability.

133 From the above brief review, we reached an understanding
 134 that regional salinity mapping and assessment require inte-
 135 grated approaches which consider multidimensional (or multi-
 136 aspect) observation and analysis from surface (e.g., vegetated
 137 and nonvegetated areas) to subsoil (within a limited depth of,
 138 e.g., <150 cm), and from multiple biophysical characterization
 139 to traditional soil sampling. We propose, hence, in this paper a
 140 “multiyear maxima and multiscale modeling” methodology for
 141 salinity quantification in Mesopotamia, Iraq.

II. MATERIALS AND METHODS

142

A. Study Area

143

Mesopotamia, “the land between rivers” in ancient Greek and
 144 encompassing a surface area of about 135 000 km², is a typ-
 145 ical alluvial plain between the two famous rivers, Euphrates
 146 and Tigris (Fig. 1) and the home of multiple ancient civiliza-
 147 tions namely Sumerian, Akkadian, Babylonian, and Assyrian
 148 [4]. As an arid subtropical region, the climate is characterized
 149 by dry hot summers and cooler winters [2], [3], [29], where
 150 annual rainfall is mostly below 200 mm, of which the average
 151 is 110 mm in Baghdad and 149 mm in Basrah in the past three
 152 decades. The mean maximum and minimum temperatures are
 153 44°C and 25.6°C, respectively, in Baghdad, 46°C and 29.15°C
 154 in Basrah in July–August, whereas they are 16.5°C and 4.8°C
 155 in Baghdad, 19°C and 8.4°C in Basrah in December–January.

156 As a fluvial plain, soils are extremely calcareous (20–30%
 157 lime) alluvial silty loam or loamy silts [2], [3], typical
 158 Fluvisols in terms of WRB (the World Reference Base for
 159 Soil Resources), and mostly saline as a result of cumula-
 160 tive salinization in the past 6000 years [2]–[4]. Archeological
 161 evidence revealed that crop cultivation (e.g., wheat and bar-
 162 ley) was started as early as 4000 BC in Mesopotamia [2],
 163 [4]. Due to aridity, farming is impossible if not irrigated.
 164 Irrigation increases soil moisture and crop production, nonethe-
 165 less, leads to elevation of water-table or water-logging in the
 166 area where there is no drainage or draining is slow [2]–[4].
 167 Consequently, salts accumulate in soils after evaporation and
 168 transpiration year by year. According to Jacobsen and Adams
 169 [4], salinity had already become a serious hazard in south-
 170 ern Mesopotamia in the late Sumerian or early Akkadian
 171 periods, e.g., around 2400–2300 BC, and led to a decline
 172 in wheat production. The proportions of wheat and barley
 173 were nearly equal in about 3500 BC but became 1 to 6
 174 in 2400 BC in Girsu (nowadays Thi-Qar); wheat cultivation
 175 was completely abandoned after 1700 BC and land produc-
 176 tivity declined from 2537 l/ha before 2400 BC to 897 l/ha in
 177 1700 BC in Larsa (also in Thi-Qar) as a consequence of salin-
 178 ization. Salinity is hence an old problem that contributed to
 179 the breakup of ancient civilization [4]. Unfortunately, saliniza-
 180 tion has never stopped but progressively extended to the whole
 181 Mesopotamian plain to the state as described in the beginning
 182 of the paper.

183 As Buringh investigated [2], the most common salt in
 184 saline soils is sodium chloride (NaCl) followed by other
 185 chlorides (e.g., CaCl₂, MgCl₂, and KCl), and sulfates (e.g.,
 186 CaSO₄·2H₂O, Na₂SO₄·10H₂O, and MgSO₄). Saline-alkaline
 187 soils may exist locally but real alkali soils (in black) are very
 188 scarce in Mesopotamia.
 189

B. Field Sampling Design and Data

190

To achieve our objectives, comprehensive observations and
 191 measurements at different scales are required. The experi-
 192 ment was hence designed to be conducted at three levels, i.e.,
 193 plot, local (pilot site), and regional scales, corresponding to
 194 the proposed multiscale approach. Both local (pilot site)- and
 195

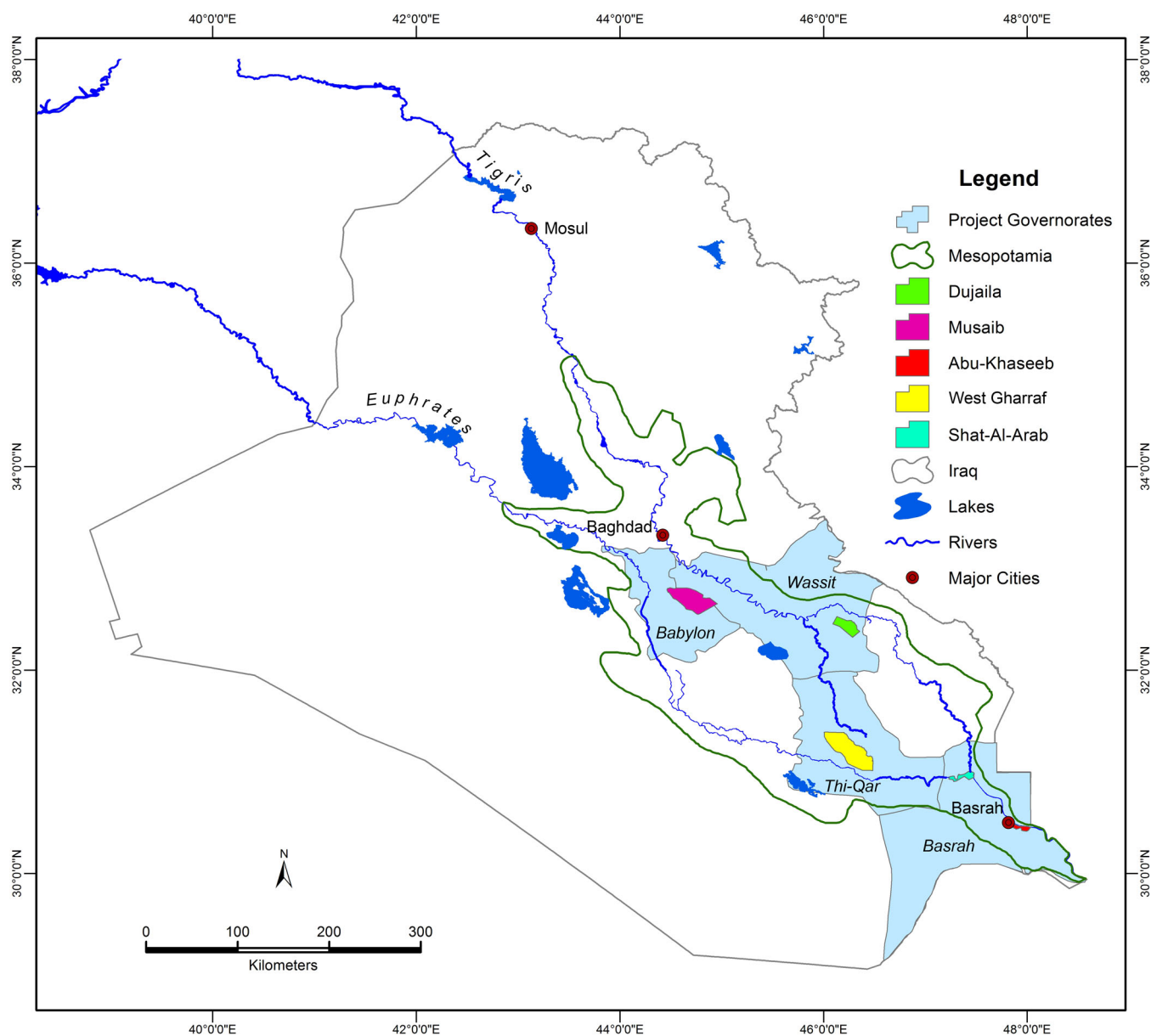


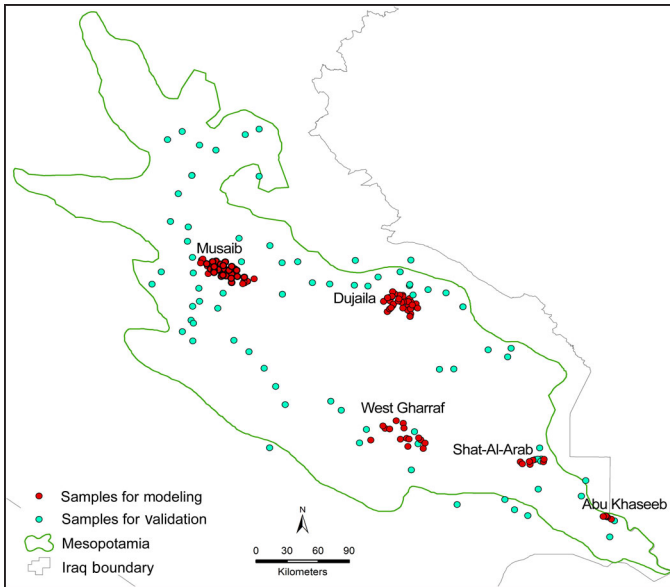
Fig. 1. Location of the five pilot sites and the whole study area, Mesopotamia, in Iraq.

196 regional-scale surveys were composed of plot level investigation
197 and measurements.

198 Plot level survey included land use/cover investigation, crop
199 types and performance observation (if possible), soil sampling,
200 and apparent salinity measurement using a ground conductivity
201 meter, EM38-MK2 (Geonics Ltd.), in an area of $1\text{ m} \times 1\text{ m}$.
202 EM38 meter is capable to measure the apparent soil salinity
203 in both horizontal (with a measurement depth up to 50 cm)
204 and vertical (up to 150 cm) directions, of which the readings
205 can be respectively denoted as EM_H (horizontal) and
206 EM_V (vertical) in millisiemens per meter (mS/m). Hence,
207 EM38 meter can reveal salinity of both surface and subsoil.
208 However, the apparent salinity has to be calibrated by laboratory
209 measured soil salinity. The false salinity caused by metal
210 and/or soil moisture should be avoided while measurement is
211 conducted.

In order to be comparable with the pixels of high-resolution
212 satellite images such as Landsat and SPOT (e.g., 10–30 m),
213 the survey was planned to be conducted in three plots distributed
214 at three corners of a triangle, respectively, with a distance of
215 about 15–20 m from each other in the same patch of land. The
216 averaged values of the EM38 readings including both EM_V and
217 EM_H of the three corner plots would be taken to represent the
218 salinity of the center of the observed triangle. Soil samples for
219 laboratory chemical analysis were to be taken from soil profiles
220 at the depth of 0–30, 50–70, 90–110 and 120–150 cm, and from
221 surface (0–30 cm in depth) using auger tools in the plots where
222 EM38 was also measured.
223

Pilot site level survey was to serve for integrated pilot
224 study, e.g., salinity model development and mapping at local
225 scale. As recommended by the Iraqi government, five sites
226 namely Musaib, Dujaila, West Gharraf, Shat-Al-Arab, and Abu
227



F2:1 Fig. 2. Distribution of the sampling points for modeling and validation.

228 Khaseeb in the Mesopotamian plain (see Figs. 1 and 2 for location)
 229 were selected for pilot studies. It was planned that each
 230 pilot site should contain >5 soil profiles and >20 triangles of
 231 plots for surface survey if accessibility allowed.

232 Regional survey, which was aimed at salinity model develop-
 233 ment and validation at regional-scale, was to be conducted
 234 along two transects in the whole Mesopotamian Plain.

235 Based on the above design, field survey and sampling cam-
 236 paigns were conducted in the five pilot sites in the period
 237 September 2011–July 2012 and along two regional transects
 238 in Mesopotamia in April 2012 and June 2013. The sampling
 239 locations for plot level survey both in pilot sites and along
 240 the regional transects were randomly selected in the field
 241 in terms of accessibility. Due to limited budget, surface soil
 242 samples were not taken in each plot but at least in one of the three
 243 corners. Soil salinity, expressed as electrical conductivity (EC)
 244 in decisiemens per meter (dS/m), was measured in laboratory
 245 using 1:1 dilution method. In total, 187 surface soil samples
 246 (0–30 cm) with laboratory analysis and 485 pairs of EM38
 247 measurements were obtained for this study. Sites, depths, and
 248 numbers of sampling are described in Table I.

249 In order to extend plot level measurements to pilot site, and
 250 then to regional-scale salinity mapping, a multiyear dataset
 251 consisting of multiresolution and multisensor satellite imagery
 252 was prepared based on the availability of images. This dataset
 253 includes 33 spring (February–April) and summer (August)
 254 Landsat ETM+ images of the period 2009–2012, four SPOT 4
 255 images acquired in March 2010, and three RapidEye images
 256 dated April 2012, time-series of MODIS vegetation indices
 257 data (MOD13Q1), and LST (MOD11A1 and A2) from 2009
 258 to 2012.

259 C. Local-Scale Modeling and Mapping

260 As indicated in Section I, apart from the geophysical survey
 261 by EM38 meter to understand salinity in surface and subsoil,

different remote sensing indicators that can characterize the
 multiaspect surface biophysical features, e.g., VIs, LST, soil
 brightness (albedo), and principal components (PCs), need to
 be derived.

262
 263
 264
 265
 266 Instead of using one single image, a 4-year imagery dataset
 267 registered both spring and summer acquisitions, which was
 268 used to derive the multiyear maximal values of a set of VIs and
 269 nonvegetation indices (NonVIs) for each pixel. This would help
 270 avoiding some false alarm of salinity arising from fallowing,
 271 crop rotation, and variation in soil moisture. This processing
 272 can also largely remove the problem caused by the image gaps
 273 left by the Scan-Line Corrector failure (SLC-Off) in the Landsat
 274 ETM+ imagery since 2003. We assumed that it is always possi-
 275 ble for a given piece of cropland to be cultivated in either spring
 276 or summer with normal performance in the observed period
 277 because fallow state lasts, in general, 2–3 years in Central and
 278 Southern Iraq.

279 Image processing in combination with field survey would
 280 allow the identification of the salt-tolerant areas, and the con-
 281 centration of salt in subsoil, for example, areas with high
 282 vegetation greenness but moderate salinity as revealed by the
 283 readings of EM 38 or as measured by soil laboratory analy-
 284 sis. Such areas have to be defined for a specific analysis since
 285 salinity cannot be reflected by vegetation indices.

286 Furthermore, it is essential to separate vegetated and non-
 287 vegetated areas, as the expression of salinity in remote sensing
 288 images is different in these two types of areas. For exam-
 289 ple, the low values of VIs in nonvegetated areas (e.g., bare
 290 soil and desert) do not mean that they are all strongly salin-
 291 ized (high salinity). As a matter of fact, salinity is negatively
 292 correlated with VIs such as NDVI [11], [13], [28], [29], and
 293 it tends to be overestimated in the nonvegetated areas just
 294 based on VI-related models. We have to consider the inte-
 295 grated information from multiple spectral and thermal bands,
 296 e.g., spectral reflectance, LST, PCs, and the brightness of
 297 the Tasseled Cap transformation (TCB) [47]–[49], for salin-
 298 ity assessment in these areas. The rationale behind is that
 299 the spectral reflectance and its multiband linear combination
 300 (e.g., TCB and PCs) together with LST might be able to
 301 highlight the subtle difference in soil brightness (or albedo)
 302 corresponding to the difference in salinity in the nonvegetated
 303 areas.

304 The procedure for local-scale study in the pilot sites is
 305 presented as follows.

- 306 1) *Atmospheric correction using FLAASH model* [50] for all
 307 Landsat ETM+, SPOT, and RapidEye images.
- 308 2) *Multispectral transformation*: A set of most frequently
 309 applied VIs such as NDVI [31], SAVI (soil-adjusted
 310 vegetation index) [51], SARVI (soil-adjusted and atmo-
 311 spherically resistant vegetation index) [52], and EVI
 312 (enhanced vegetation index) [53] were produced from
 313 the atmospherically corrected and reflectance-based satel-
 314 lite imagery. We also introduced a new vegetation index
 315 in this work, the generalized difference vegetation index
 316 (GDVI) developed by Wu [54] and in the form of

$$GDVI = (\rho_{NIR}^n - \rho_R^n) / (\rho_{NIR}^n + \rho_R^n) \quad (1)$$

T1:1
T1:2TABLE I
LOCATION, DEPTH, AND NUMBER OF SOIL SAMPLES AND EM38 MEASUREMENTS

Pilot sites	Number of soil profile (0–150 cm)	Number of surface soil samples (0–30 cm)			Number of EM38 readings	
		Sep. 2011–Apr. 2012	Supplemental Jun.–Jul. 2012	Jun. 2013	Mar.–Apr. 2012	Supplemental Jun.–Jul. 2012
Musaib	13	30	6		45	23
Dujaila	5	17	6		65	17
West Gharraf		22	4		57	17
Shat-Al-Arab	4	8			54	
Abu Khaseeb	5				15	
Transects						
Transect 1-North		26		13	60	
Transect 2-South		44		11	132	
Total	27		187		485	

where ρ_{NIR} is the reflectance of the near-infrared band and ρ_R is that of the red band, and n is the power, an integer from 1 to n . When $n = 1$, GDVI = NDVI. As Wu concluded [54], when $n = 2$, GDVI is better correlated with LAI (leaf area index) in all biomes, and more sensitive to low vegetated biomes than other vegetation indices. However, with the increase of n (e.g., $n = 3$ and 4), GDVI becomes saturated and insensitive to densely vegetated areas (e.g., wheat cropland, forest). High-power GDVI is thence only relevant for application in sparsely vegetated dryland biomes (such as rangeland and woodland). Our earlier studies show that GDVI is a powerful salinity indicator [28], [29], [55]. We applied this index ($n = 2$) together with others in soil salinity modeling and mapping in this study.

Regarding NonVIs, as well as NDII (normalized difference infrared index) [56], TCB, PC1, and PC2, LST were derived from Landsat ETM+ images.

3) *Derivation of the multiyear maxima of VI and nonVI images:* An algorithm using IDL language was designed for this purpose. The multiyear maxima of VIs and NonVIs of the period of 2009–2012 were derived for each pixel in all pilot sites. For NonVIs, multiyear spring maxima, i.e., the maxima during the crop growing period from February 01 to April 15 (note: barley is harvested in the end of April) were also produced.

We have to mention that SPOT and RapidEye images do not contain any thermal band to derive LST and thus cannot be individually used for salinity modeling in our study. After resampling the pixels to 30 m, their VIs (NDVI, SAVI, and GDVI) and NonVIs (PC1 and PC2) were integrated into those of Landsat ETM+ to derive the maxima of VIs and NonVIs in each pixel.

4) *Extraction of the maxima of each VI and nonVI corresponding to the field sampling locations:* Both maximal images of VIs and NonVIs were converted into TIF format, and imported into ArcGIS to extract the maximal values corresponding to each sampling plot location.

5) *Division of the vegetated and nonvegetated areas:* A thresholding technique was applied to the

multiyear-maximal NDVI to determine the threshold for division of the vegetated and nonvegetated areas followed by a mask operation.

6) *Linking multiyear maxima with plot-scale measurements:* The extracted maxima of VIs and NonVIs were coupled with their correspondingly averaged plot-level EM38 readings or laboratory-measured soil electrical conductivity using SYSTAT, a software for statistical analysis and modeling, for salinity model development using multiple linear regression analysis at the confidence level of 95%. A positive correlation between salinity and LST, PCs and TCB, and a negative correlation between salinity and different VIs, especially GDVI and NDVI, were observed.

Two types of salinity models were obtained: a) specific salinity models for vegetated and nonvegetated areas resulted from multiple linear regression modeling that was applied to two groups of samples located in vegetated and nonvegetated areas and b) integrated salinity models in which all samples in the same pilot site were input for modeling but vegetated and nonvegetated areas were separately treated.

7) *Evaluation and application of the salinity models:* To understand whether the models obtained are operational, the specific and integrated models were, respectively, applied back to the maxima of VIs and NonVIs of the period 2009–2012 to produce local-scale salinity maps. These maps were evaluated against the ground-measured data by linear regression model [29], [34]. If the agreement between the measured and predicted salinity is $\geq 80\%$, the models developed are considered operational at local-scale and the salinity maps are reliable.

D. Regional-Scale Mapping

1) *Regional-scale modeling:* Models obtained from any pilot site cannot be directly applied to regional-scale salinity mapping due to lack of spatial representativeness. That is why we proposed here a “multiscale modeling” approach to upscale plot-level measurements

317
318
319
320
321
322
323
324
325
326
327
328
329
330
331
332
333
334
335
336
337
338
339
340
341
342
343
344
345
346
347
348
349
350
351
352
353
354
355
356357
358
359
360
361
362
363
364
365
366
367
368
369
370
371
372
373
374
375
376
377
378
379
380
381
382
383
384
385
386
387
388
389
389
390
391
392
393
394

TABLE II
SALINITY MODELS FOR THE PILOT SITES AND THE WHOLE MESOPOTAMIA

Scale	Type	Salinity models	Error scope	Multiple R ²		
<i>Pilot</i>	Musaib	Vegetated area	$EM_V = -824.134 + 918.536*GDVI - 754.204*\ln(GDVI)$	± 41.700	0.925	
		Nonvegetated area	$EM_H = -606.197 - 460.043*\ln(GDVI) + 245.086*\exp(GDVI)$	± 48.559	0.862	
	<i>Site scale</i>	Dujaila	Vegetated area	$EM_V = 535.403 - 487.905*GDVI$	± 64.168	0.729
			Nonvegetated area	$EM_V = -2725.05 + 10.018*LST - 509.494*NDII$	± 73.23	0.650
		West Gharraf	Vegetated area	$EM_V = -78.811 - 353.217*\ln(GDVI)$	± 143.992	0.684
			Nonvegetated area	$EM_V = -19337.102 + 63.795*LST$	± 166.515	0.578
<i>Regional scale</i>		Vegetated area	$EM_V = 66.338 - 258.114*\ln(GDVI)$	± 88.882	0.717	
		Nonvegetated area	$EM_V = 3055497.34 + 2161.09*LST - 649347.93*\ln(LST)$	± 92.524	0.695	

Note: EM_V and EM_H can be converted into EC (dS/m) from the regional transect sampling, i.e., $EC = 0.0005EM_V^2 - 0.0779EM_V + 12.655$ ($R^2 = 0.8505$); and $EC = 0.0002EM_H^2 + 0.0956EM_H + 0.0688$ ($R^2 = 0.7911$).

395 and high-resolution-derived models to regional-scale
396 assessment. To do so, the data from different pilot sites,
397 which are situated in different locations in Mesopotamia
398 (Fig. 2), were integrated together for regional-scale mod-
399 eling using the same multiple regression model.

400 2) *Upscaling test and regional salinity mapping*: Since we
401 will use MODIS data (VIs and LST) for regional salinity
402 mapping, it is still not clear whether the models devel-
403 oped from high-resolution data (e.g., Landsat and SPOT)
404 are applicable to MODIS data. For this reason, the best
405 salinity indicators as revealed in the previous steps, the
406 multiyear maxima of GDVI, and the LST maxima of the
407 crop growing period from February to April in 2009–
408 2012 (of the frame 168-37) were linked, respectively, to
409 the multiyear maxima of MODIS GDVI (calculated from
410 MOD13Q1), and the maximal LST (MOD11A2) of the
411 same period after resolution degradation of the Landsat
412 data from 30 to 250 m and upgrading of LST data from
413 1000 m to 250 m. This processing was aimed at minimiz-
414 ing the information loss or unrealistic improvement [54].
415 1000 random points covering all land cover types such
416 as barelands (deserts, bare soils, and bare rocks), saline
417 soils, urban areas, rangeland, and croplands were gener-
418 ated. By removing those falling in roads and swamps, it
419 was found that Landsat GDVI ($GDVI_L$) is strongly corre-
420 lated with MODIS GDVI ($GDVI_M$) [$R^2 = 0.839$ in (2)],
421 and the same was obtained for Landsat LST and MODIS
422 LST [$R^2 = 0.795$ in (3)]

$$\begin{aligned} GDVI_M &= 0.7837GDVI_L + 0.1665 \text{ or } GDVI_L \\ &= (GDVI_M - 0.1665)/0.7837 \end{aligned} \quad (2)$$

$$\begin{aligned} LST_M &= 0.7054LST_L + 90.496 \text{ or } LST_L \\ &= (LST_M - 90.496)/0.7054 \end{aligned} \quad (3)$$

423
424 Therefore, with relevant adjustment of MODIS GDVI and
425 LST in line with (2) and (3), regional models developed
426 from high resolution Landsat data are applicable to the
427 adjusted MODIS data for regional salinity mapping.

428 For such upscaling test, one may also propose the same
429 random processing for multiple Landsat scenes against
430 MODIS data to get the average to evaluate the extendabil-
431 ity. Since the land cover types are the same in the region,
432 the results should be more or less similar to what we have
433 obtained.

434 3) *Validation*: The regional salinity map derived from the
435 MODIS data was evaluated against the field samples from
436 two regional transects (blue points in Fig. 2) to check its
437 reliability and accuracy.

III. RESULTS AND DISCUSSION

438
439 After the above processing, both local- and regional-scale
440 salinity models obtained are listed in Table II, and local-scale
441 and regional-scale salinity maps are presented in Figs. 3 and 4
442 for discussion.

A. Salinity Models and Maps

443
444 As our test revealed in the Dujaila site [29], specific models
445 for vegetated and nonvegetated areas were not recommended
446 for salinity mapping due to their low reliability (e.g., < 37%).
447 Thus, what are presented in Table II are the integrated mod-
448 els taking all the samples into account, whereas vegetated and
449 nonvegetated areas were separated during the multiple linear
450 regression analysis in each pilot site. We see that among all
451 the VIs, GDVI or its variant such as $\ln(GDVI)$ is the most rep-
452 resentative indicator for vegetated areas, and LST (and NDII)
453 for nonvegetated areas in all pilot sites. By the way, for sites
454 Shat-Al-Arab and Abu Khaseeb, independent models were
455 not developed due to limited soil sample number (8 and 5,
456 respectively).

457 It is also noted that the salinity models obtained are different
458 from each other in all pilot sites; none of them can be directly
459 extended to regional-scale mapping due to spatial variability.
460 However, these models can reliably predict soil salinity with
461 an accuracy of about 82.57% in Dujaila and 83.01% in Musaib
462 against the field measured data. Hence, they were considered
463 operational for their respective pilot sites.

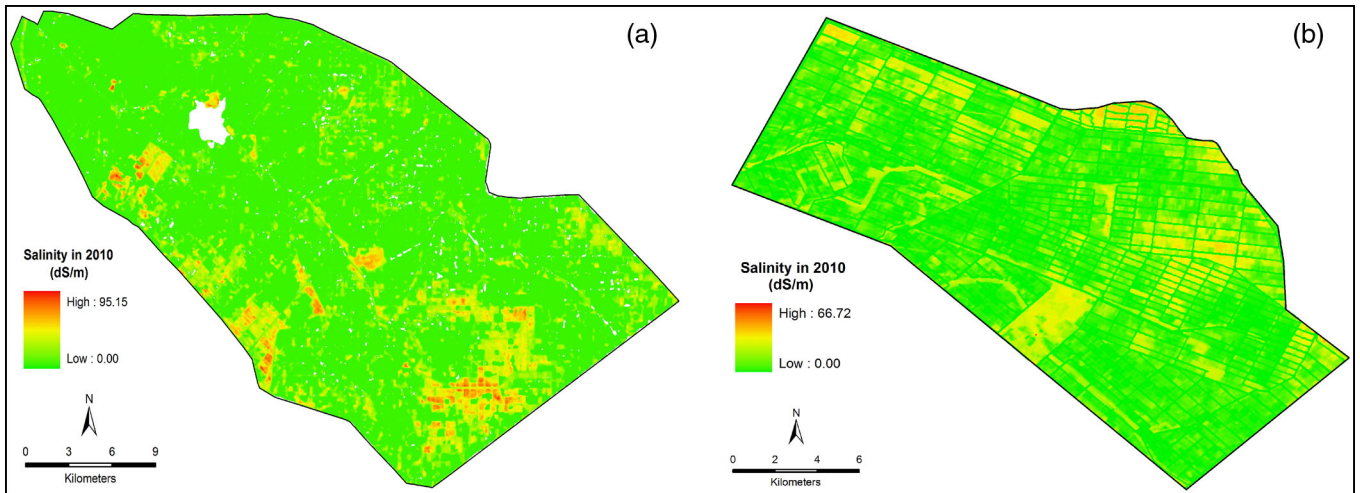
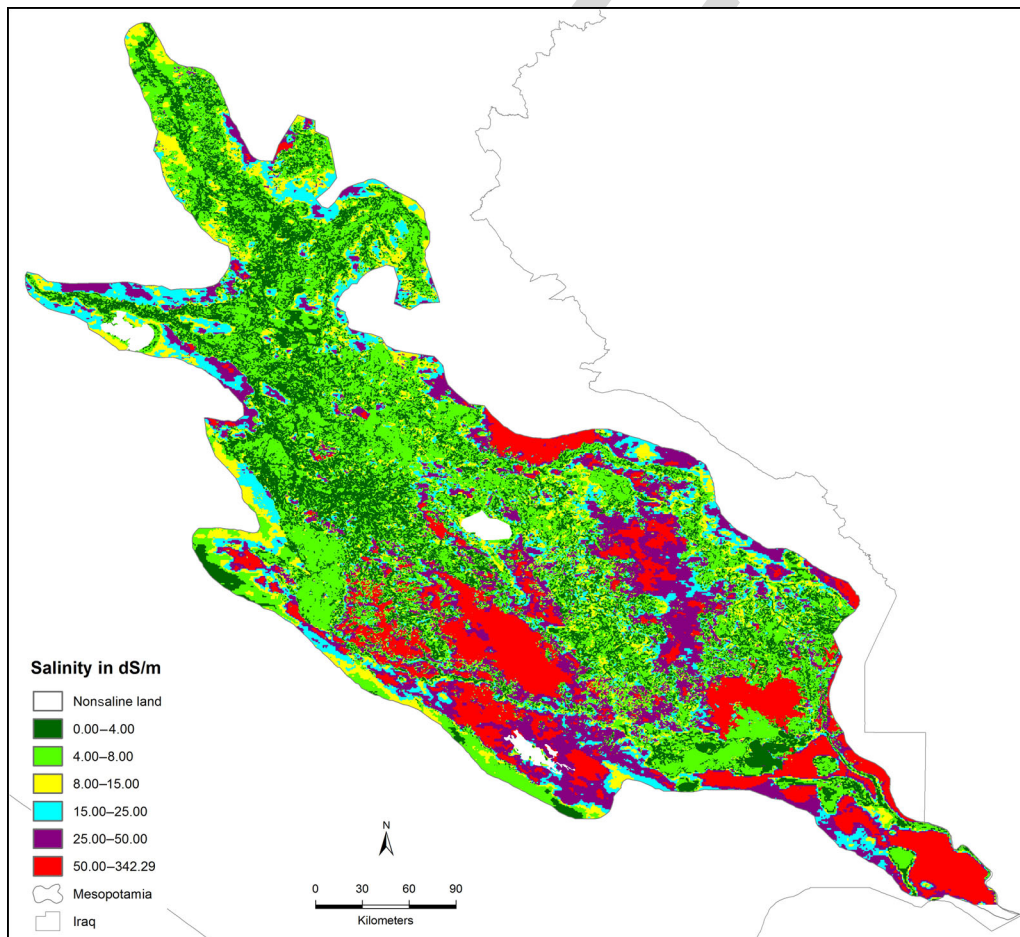


Fig. 3. Salinity of the pilot sites: (a) Musaib and (b) Dujaila.

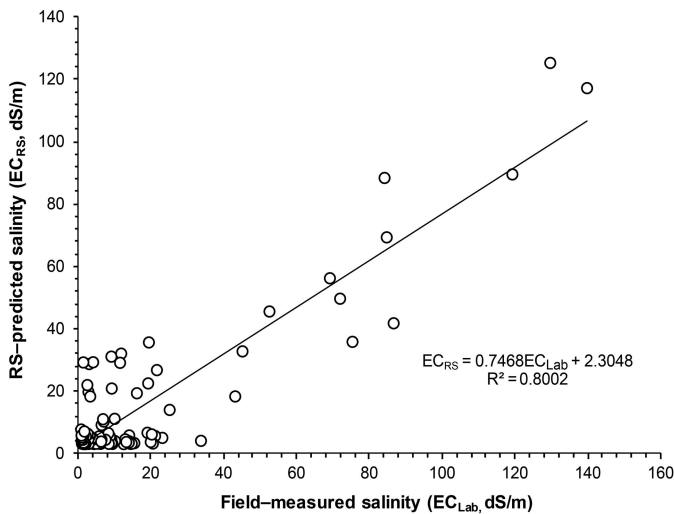
F3:1



F4:1 Fig. 4. Present-state salinity map of Mesopotamia (expressed in EC classes as required by users).

464 For the regional-scale models, the multiple correlation coef-
 465 ficients R^2 are relatively lower than those in pilot sites due to
 466 homogenization of samples from different pilot sites after inte-
 467 gration; nonetheless, they have higher applicability in regional-
 468 scale mapping.

It is worth mentioning that most of the EM38 measurements 469
 in spring (March–April) 2012 did not show any promising cor- 470
 relation with VIs except for the Dujaila site perhaps due to 471
 the problem of soil moisture after rainfall or irrigation while 472
 measurements were undertaken in the field. For this reason, a 473



F5:1 Fig. 5. Agreement of the remote sensing-predicted salinity (EC_{RS}) versus
 F5:2 field-measured salinity (EC_{Lab}).

474 supplemental sampling campaign was carried out in the dry
 475 season after crops harvesting (June–July 2012). These EM38
 476 readings show a good correlation with the multiyear maximal
 477 VIs and NonVIs in all pilot sites and were used for develop-
 478 ing salinity models by multiple linear regression analysis. NDII
 479 and LST are of both vegetation and nonvegetation characters,
 480 and were included in the integrated salinity modeling for both
 481 vegetated and nonvegetated areas.

482 The local salinity maps of the present-state taking the sites
 483 Musaib and Dujaila as an example [Fig. 3(a) and (b)] are in a
 484 good agreement with ground data ($R^2 = 0.830$ in Musaib, and
 485 0.826 in Dujaila). We consider that these maps are reliable.

486 As for the regional salinity map (Fig. 4), the accuracy eval-
 487 uation revealed that 23 of the 121 regional samples taken along
 488 two transects and the surface EC of 27 soil profiles in pilot sites
 489 that were not used for modeling were abnormal due to inter-
 490 nal problem of samples, most probably, derived from laboratory
 491 analysis (because the correlation among Cl^- , Na^+ , and EC is
 492 very low, e.g., $R^2 = 0.047$); however, the remaining 98 samples
 493 show a good accordance with remote sensing predicted salinity.
 494 The observation accuracy is 80.9%, and the statistical accuracy
 495 of the regional salinity map obtained by linear regression analy-
 496 sis at the confidence level of 95% is 80.02% (Fig. 5). Therefore,
 497 the regional map presented in Fig. 4 was considered reliable.

498 The agreement between the measured and remote sensing
 499 predicted salinity as shown in Fig. 5 is higher in the high salin-
 500 ity part than low salinity one. This is probably due to the fact
 501 that coarse-resolution LST has lower sensitivity to low salin-
 502 ity. An overestimation of about 2–10 dS/m may occur in some
 503 places in the weakly salinized areas. However, the sensitivity
 504 to low salinity can be improved if high resolution LST data are
 505 available.

506 One may have concern about the reasonability to use soil
 507 surface temperature, LST, as salinity indicator which was
 508 finally retained in the models for the nonvegetated areas. As
 509 Wu *et al.* [29] argued, it is commonly known that thermal
 510 conductivity of materials is temperature (T)-dependent, and
 511 the former is associated with electrical conductivity (EC).

512 However, the interrelationship between the thermal and
 513 electrical conductivities is complex and may change signifi-
 514 cantly depending on materials, e.g., soil types. Some authors
 515 [5]–[7] have explored the possibility to use the thermal band
 516 to identify the salt-affected soils but they have not discussed
 517 the mechanism behind. Abu-Hamdeh and Reeder [57] ascer-
 518 tained the relationship between thermal conductivity and salin-
 519 ity, and found that thermal conductivity decreases with the
 520 increase in the amount of added salts at given moisture content.
 521 Sepaskhah and Boersma [58] found that the apparent thermal
 522 conductivity is independent of water content at very low water
 523 contents. Consequently, in driest condition (at lowest moisture
 524 or water content), thermal conductivity is associated with the
 525 salt amount—salinity. We believe, therefore, that LST-based
 526 models are relevant for mapping salinity in nonvegetated areas.

527 Concern may also be addressed on the applicability of the
 528 models. It is clear that the models obtained from pilot sites
 529 are not recommended for direct application to similar areas for
 530 salinity mapping without relevant adaptation. Of higher repre-
 531 sentativeness, the regional-scale models can be disseminated to
 532 the similar environment for this purpose.

B. Assessment of the Integrated Processing Approach

533 Different from the other authors (e.g., [10], [17], and [18]),
 534 we used multiyear imagery dataset to derive the multiyear
 535 maxima of VIs and NonVIs for multiscale salinity model-
 536 ing followed with an upscaling analysis. The above-mentioned
 537 problematic issues that are commonly faced in salinity mapping
 538 by remote sensing were successfully minimized, and salinity
 539 maps with high reliability were produced.

540 Despite a number of authors [10], [17] have conducted salin-
 541 ity mapping and best band combination studies, but they used
 542 single or multiple single images and did not differently treat the
 543 vegetated and nonvegetated areas. Especially, authors [17] did
 544 not take into account the nonvegetated area. Their approaches
 545 cannot avoid the influences from crop rotation/fallow, and
 546 moisture, which are often problematic in large area (or scale)
 547 mapping. Hence, our approach has evident advantages over and
 548 its uniqueness different from others.

549 However, some imperfection was also noted. As a matter
 550 of fact, salinity has strong spatial variability; even in a small
 551 $1 \times 1 \text{ m}^2$ plot, salinity may change after each 20–30 cm inter-
 552 val, not to mention in the 250 m pixels of MODIS data which
 553 were used for regional-scale mapping in this study. That is to
 554 say, it is unlikely to produce a regional salinity map with an
 555 accuracy of 2–3 dS/m based on the proposed methodology.
 556 What can be done is to approach the reality as much as possible
 557 by increasing the sampling number and density with a relevant
 558 spatial distribution if both time and fund are available.

C. Problems Confronted

560 Though great efforts have been made, problem related to salt-
 561 tolerant vegetation has not been completely resolved yet. In the
 562 pilot sites, field sampling was well conducted and halophytes
 563 were noted. But in other areas where sampling was not covered,
 564 salinity may have been underestimated as salt-tolerant crops
 565

566 such as barley or other halophyte vegetation were not identified
567 out for specific analysis. As was revealed by the experiment
568 [3], barley has a rather strong resistance to salinity, and can
569 still grow well with good production (1.68–1.84 tons/ha) in the
570 field where soil salinity reaches 8–16 dS/m if fertilizer (e.g.,
571 nitrogen) is given.

572 The second issue is related to swamps and their surroundings,
573 e.g., in the governorates of Thi-Qar and Basrah of Southern Iraq
574 (Fig. 1). Moisture is almost a permanent problem for salinity
575 mapping in these areas. Swamps can be excluded out for any
576 salinity analysis but their surroundings are mostly moist veg-
577 etated area (locally cropland but mostly halophytes). In this
578 mapping work, we tried to find the transitional part between
579 moist (>345 dS/m, the false salinity as LST model loses its
580 sensitivity with increase of moisture) and nonmoist zones
581 (<345 dS/m), and then treated the moist part as normal water
582 body or swamp.

583 The third problematic issue is related to bareland. Due to
584 security reasons, a number of sampling plots designed in the
585 nonvegetated areas were not accessible. There were not enough
586 samples from bare soil for model development and salinity map
587 validation. Thus both salinity models and maps of the non-
588 vegetated areas should be improved when security condition
589 improves and more field data become available.

590 IV. CONCLUSION

591 In spite of challenges, this study demonstrates the possibility
592 to map and quantify the spatial distribution of the salt-affected
593 land at regional-level based on the development of local- and
594 regional-scale salinity models in Mesopotamia, Iraq. The val-
595 idated maps we produced can be tentatively provided as a
596 reference to decision-makers for facilitating their future land
597 use planning in Mesopotamia. The proposed method can mini-
598 mize the problems related to crop rotation/fallow practices, and
599 soil moisture, and hence is different from other approaches. The
600 models can be applied for multitemporal salinity mapping to
601 track the temporal and spatial changes in the Mesopotamian
602 plain and even in the whole country.

603 However, one weak point is noted, i.e., the approach can-
604 not completely remove the influence from salt-tolerant crops
605 such as barley, alfalfa, and cotton in the areas where no field
606 survey was conducted. In addition, coarse resolution LST data
607 (1000 m) is really not ideal for such quantification as spatial
608 variability of salinity has been greatly homogenized. Merely,
609 these issues can be sorted out or improved when new thermal
610 data with higher resolution (e.g., 60–250 m) are available, and
611 field accessibility is improved.

612 In future work, as mentioned in the introduction, ET, as one
613 of the indicators, can be taken into account together with others.
614 In this way, remote sensing-based salinity models will be more
615 comprehensive and relevant for both local- and regional-scale
616 assessments.

617 ACKNOWLEDGMENT

618 The study was financially supported by ACIAR (Australian
619 Center for International Agricultural Research) and the Italian

Government. The authors would like to thank Dr. M. Qadir 620
(UNU-INWEH), Mr. A. Platonov (IWMI-Tashkent), Dr. E. 621
Christen (CSIRO), and Dr. T. Oweis (ICARDA) for their coop- 622
eration in the early stage of the work; Dr. A. A. Hameed, 623
Dr. H. H. Al-Musawi (Ministry of Water Resources of Iraq), 624
and Dr. K. A. Saliem (Ministry of Agriculture of Iraq) for their 625
cooperation in field sampling; and Ms. B. Dardar (ICARDA) 626
for her assistance in a part of image processing. 627

REFERENCES 628

- [1] FAO, *Country Pasture/Forage Resource Profiles: Iraq*, Rome, FAO, 2011, 629
34pp. 630
- [2] P. Buringh, *Soils and Soil Conditions in Iraq*. Baghdad, Iraq: Ministry of 631
Agriculture of Iraq, 1960, 337pp. 632
- [3] P. J. Dieleman, Ed., *Reclamation of Salt Affected Soils in Iraq*. 633
Wageningen, The Netherlands: International Institute for Land 634
Reclamation and Improvement/Wageningen Publication, 1963, 175pp. 635
- [4] T. Jacobsen and R. M. Adams, "Salt and silt in ancient Mesopotamian 636
agriculture," *Science*, vol. 128, pp. 1251–1258, 1958. 637
- [5] B. Mougnot, M. Pouget, and G. Epema, "Remote sensing of salt-affected 638
soils," *Remote Sens. Rev.*, vol. 7, pp. 241–259, 1993. 639
- [6] J. A. Zinck, "Monitoring salinity from remote sensing data," in *Proc. 1st 640
Workshop Eur. Assoc. Remote Sens. Lab. (EARSeL)*, Ghent University, 641
Belgium, 2001, pp. 359–368. 642
- [7] G. I. Metternicht and J. A. Zinck, "Remote sensing of soil salinity: 643
Potentials and constraints," *Remote Sens. Environ.*, vol. 85, pp. 1–20, 644
2003. 645
- [8] J. Farifteh, A. Farshad, and R. J. George, "Assessing salt-affected soils 646
using remote sensing, solute modelling, and geophysics," *Geoderma*, 647
vol. 130, no. 3–4, pp. 191–206, 2006. 648
- [9] M. D. Steven, T. J. Malthus, F. M. Jaggard, and B. Andrieu, "Monitoring 649
responses of vegetation to stress," in *Proc. 18th Annu. Conf. Remote Sens. 650
Soc. Remote Sens. Res. Oper.*, U.K., 1992, pp. 369–377. 651
- [10] M. Zhang, S. Ustin, E. Rejmankova, and E. Sanderson, "Monitoring 652
Pacific coast salt marshes using remote sensing," *Ecol. Appl.*, vol. 7, 653
pp. 1039–1053, 1997. 654
- [11] P. Brunner, H. T. Li, W. Kinzelbach, and W. P. Li, "Generating soil elec- 655
trical conductivity maps at regional level by integrating measurements 656
on the ground and remote sensing data," *Int. J. Remote Sens.*, vol. 28, 657
pp. 3341–3361, 2007. 658
- [12] T. Zhang *et al.*, "Using hyperspectral vegetation indices as a proxy to 659
monitor soil salinity," *Ecol. Indic.*, vol. 11, pp. 1552–1562, 2011. 660
- [13] C. L. Wiegand, J. D. Rhoades, D. E. Escobar, and J. H. Everitt, 661
"Photographic and videographic observations for determining and map- 662
ping the response of cotton to soil salinity," *Remote Sens. Environ.*, 663
vol. 49, pp. 212–223, 1994. 664
- [14] N. Fernández-Buces, C. Siebe, S. Cram, and J. L. Palacio, "Mapping soil 665
salinity using a combined spectral response index for bare soil and vegeta- 666
tion: A case study in the former lake Texcoco, Mexico," *J. Arid Environ.*, 667
vol. 65, pp. 644–667, 2006. 668
- [15] D. B. Lobell, J. I. Ortiz-Monasterio, F. C. Gurrola, and L. Valenzuela, 669
"Identification of saline soils with multiyear remote sensing of crop 670
yields," *Soil Sci. Soc. Amer. J.*, vol. 71, pp. 777–783, 2007. 671
- [16] J. A. Poss, W. B. Russell, and C. M. Grieve, "Estimating yields of salt- 672
and water-stressed forages with remote sensing in the visible and near 673
infrared," *J. Environ. Qual.*, vol. 35, pp. 1060–1071, 2006. 674
- [17] R. S. Dwivedi and B. R. M. Rao, "The selection of the best possible 675
Landsat TM band combination for delineating salt-affected soils," *Int. J. 676
Remote Sens.*, vol. 13, pp. 2051–2058, 1992. 677
- [18] A. A. Eldeiry and L. A. Garcia, "Comparison of ordinary kriging, regres- 678
sion kriging, and cokriging techniques to estimate soil salinity using 679
Landsat images," *J. Irrig. Drain. Eng.*, vol. 136, pp. 355–364, 2010. 680
- [19] D. W. Roberts, T. I. Dowling, and J. Walker, "FLAG: Fuzzy landscape 681
analysis GIS method for dryland salinity assessment," CSIRO, Australia, 682
Tech. Rep. No 8/97, 1997 [Online]. Available: [http://www.clw.csiro.au/
publications/technical97/tr8-97.pdf](http://www.clw.csiro.au/publications/technical97/tr8-97.pdf), accessed on Oct. 2013 683
684
- [20] G. Metternicht, "Assessing temporal and spatial changes of salinity using 685
fuzzy logic, remote sensing and GIS. Foundations of an expert system," 686
Ecol. Model., vol. 144, pp. 163–177, 2001. 687
- [21] D. Malins and G. Metternicht, "Assessing the spatial extent of dryland 688
salinity through fuzzy modeling," *Ecol. Model.*, vol. 193, pp. 387–411, 689
2006. 690

- 691 [22] W. Wu, "Monitoring land degradation in drylands by remote sensing," in
692 *Desertification and Risk Analysis Using High and Medium Resolution*
693 *Satellite Data*, A. Marini and M. Talbi, Eds. New York, NY, USA:
694 Springer, 2009, pp. 157–169.
- 695 [23] G. Metternicht, "Analysing the relationship between ground based
696 reflectance and environmental indicators of salinity processes in the
697 Cochabamba Valleys (Bolivia)," *Int. J. Ecol. Environ. Sci.*, vol. 24,
698 pp. 359–370, 1998.
- 699 [24] R. L. Dehaan and G. R. Taylor, "Field-derived spectra of salinized
700 soils and vegetation as indicators of irrigation-induced soil salinization,"
701 *Remote Sens. Environ.*, vol. 80, pp. 406–417, 2002.
- 702 [25] J. Farifteh, F. van der Meer, C. Atzberger, and E. Carranza, "Quantitative
703 analysis of salt-affected soil reflectance spectra: A comparison of two
704 adaptive methods (PLSR and ANN)," *Remote Sens. Environ.*, vol. 110,
705 pp. 59–78, 2007.
- 706 [26] L. Garcia, A. Eldeiry, and A. Elhaddad, "Estimating soil salinity using
707 remote sensing data," in *Proc. Central Plain Irrig. Conf.*, 2005, pp. 1–10
708 [Online]. Available: <http://www.ksre.ksu.edu/irrigate/OOW/P05/Garcia.pdf>,
709 accessed on Jan. 2013.
- 710 [27] L. Garcia, A. Elhaddad, J. Chavez, and J. Altenhofen, "Remote sensing
711 to improve ET estimates," Presented at the *Evapotranspiration Workshop*
712 *Using Best Sci. Estimate Consumptive Use*, Fort Collins, CO, USA,
713 Mar. 12, 2010 [Online]. Available: http://ccc.atmos.colostate.edu/ET_Workshop/pdf/12_Garcia.pdf,
714 accessed on Dec. 2012.
- 715 [28] A. S. Mhaimeed, et al., "Use remote sensing to map soil salinity in the
716 Musaib Area in Central Iraq," *Int. J. Geosci. Geomatics*, vol. 1, no. 2,
717 pp. 34–41, 2013, ISSN 2052–5591.
- 718 [29] W. Wu et al., "Mapping soil salinity changes using remote sensing in
719 Central Iraq," *Geoderma Regional*, vol. 2–3, pp. 21–31, 2014, doi: 10.
720 1016/j.geodrs.2014.09.002.
- 721 [30] B. Rao et al., "Spectral behaviour of salt-affected soils," *Int. J. Remote*
722 *Sens.*, vol. 16, pp. 2125–2136, 1995.
- 723 [31] J. W. Rouse, R. H. Haas, J. A. Schell, and D. W. Deering, "Monitoring
724 vegetation systems in the Great plains with ERTS," in *Proc. 3rd ERTS-1*
725 *Symp., NASA SP-351*, 1973, vol. 1, pp. 309–317.
- 726 [32] B. N. Holben, "Characteristics of maximum-value composite images for
727 temporal AVHRR data," *Int. J. Remote Sens.*, vol. 7, pp. 1435–1445,
728 1986.
- 729 [33] C. J. Tucker, C. L. Vanpraet, M. J. Sharman, and G. van Ittersum,
730 "Satellite remote sensing of total herbaceous biomass production in the
731 Senegalese Sahel: 1980–1984," *Remote Sens. Environ.*, vol. 17,
732 pp. 232–249, 1985.
- 733 [34] W. Wu, E. De Pauw, and U. Hellden, "Assessing woody biomass in
734 African tropical savannahs by multiscale remote sensing," *Int. J. Remote*
735 *Sens.*, vol. 34, pp. 4525–4529, 2013.
- 736 [35] W. Wu, E. De Pauw, "Policy impacts on land degradation: Evidence
737 revealed by remote sensing in western Ordos, China," in *Land*
738 *Degradation and Desertification: Assessment, Mitigation and*
739 *Remediation*, P. Zdruli et al., Eds. New York, NY, USA: Springer,
740 2010, pp. 219–232.
- 741 [36] J. Evans and R. Geerken, "Discrimination between climate and human-
742 induced dryland degradation," *J. Arid Environ.*, vol. 57, no. 4, pp. 535–
743 554, 2004.
- 744 [37] W. Wu, E. De Pauw, and C. Zucca, "Use remote sensing to assess impacts
745 of land management policies in the Ordos rangelands in China," *Int. J.*
746 *Digit. Earth*, vol. 6, Suppl. 2, pp. 81–102, 2013.
- 747 [38] F. N. Kogan, "Application of vegetation index and brightness temperature
748 for drought detection," *Adv. Space Res.*, vol. 11, pp. 91–100, 1995.
- 749 [39] F. N. Kogan, "Global drought watch from space," *Bull. Amer. Meteorol.*
750 *Soc.*, vol. 78, pp. 621–636, 1997.
- 751 [40] Y. Bayarjargal et al., "A comparative study of NOAA–AVHRR derived
752 drought indices using change vector analysis," *Remote Sens. Environ.*,
753 vol. 105, pp. 9–22, 2006.
- 754 [41] R. R. Gillies and T. N. Carlson, "Thermal remote sensing of surface soil
755 water content with partial vegetation cover for incorporation into climate
756 models," *J. Appl. Meteorol.*, vol. 34, pp. 745–756, 1995.
- 757 [42] J. D. Kalma, T. R. McVicar, and M. F. McCabe, "Estimating land surface
758 evaporation: A review of methods using remotely sensed surface
759 temperature data," *Surv. Geophys.*, vol. 29, no. 4–5, pp. 421–469, 2008.
- 760 [43] C. R. Hain, J. R. Mecikalski, and M. C. Anderson, "Retrieval of an
761 available water-based soil moisture proxy from thermal infrared remote
762 sensing. Part I: Methodology and validation," *J. Hydrometeorol.*, vol. 10,
763 pp. 665–683, 2009.
- 764 [44] H. Qiu. (2006). *Thermal Remote Sensing of Soil Moisture: Validation of*
765 *Presumed Linear Relation Between Surface Temperature Gradient and*
766 *Soil Moisture Content* [Online]. Available: [http://people.eng.unimelb.edu.
767 au/jwalker/theses/HuangQui.pdf](http://people.eng.unimelb.edu.au/jwalker/theses/HuangQui.pdf), accessed on Aug. 2013.
- 768 [45] N. C. Coops and R. H. Waring, "The use of multiscale remote sens-
769 ing imagery to derive regional estimates of forest growth capacity using
770 3-PGS," *Remote Sens. Environ.*, vol. 75, pp. 324–334, 2001.
- 771 [46] I. Chaubey, K. Cherkauer, M. Crawford, and B. Engel, "Multiscale sens-
772 ing and modeling frameworks: Integrating field to continental scales,"
773 *Bridge*, vol. 41, pp. 39–49, 2011.
- 774 [47] R. J. Kauth and G. S. Thomas, "The Tasseled cap—A graph descrip-
775 tion of the spectral-temporal development of agricultural crops as seen
776 by Landsat," in *Proc. 2nd Int. Symp. Mach. Process. Remote Sens. Data*,
777 Purdue University, West Lafayette, IN, USA, 1976, pp. 4B41–4B51.
- 778 [48] E. P. Crist and R. C. Cicone, "Application of the tasseled cap concept
779 to simulated thematic mapper data," *Photogramm. Eng. Remote Sens.*,
780 vol. 50, pp. 343–352, 1984.
- 781 [49] C. Huang, B. Wylie, L. Yang, C. Homer, and G. Zylstra, "Derivation of
782 a tasseled cap transformation based on Landsat 7 at-satellite reflectance,"
783 *Int. J. Remote Sens.*, vol. 23, pp. 1741–1748, 2002.
- 784 [50] M. W. Matthew et al., "Status of atmospheric correction using a
785 MODTRAN4-based algorithm," in *Proc. SPIE Algor. Multispectral*
786 *Hyperspectral Ultraspectral. Imagery VI*, 2000, vol. 4049, pp. 199–207.
- 787 [51] A. R. Huete, "A soil adjusted vegetation index (SAVI)," *Remote Sens.*
788 *Environ.*, vol. 25, pp. 295–309, 1988.
- 789 [52] Y. J. Kaufman and D. Tanré, "Atmospherically resistant vegetation index
790 (ARVI) for EOS-MODIS," *IEEE Trans. Geosci. Remote Sens.*, vol. 30,
791 no. 2, pp. 261–270, Mar. 1992.
- 792 [53] A. R. Huete, H. Q. Liu, K. Batchily, and W. van Leeuwen, "A comparison
793 of vegetation indices global set of TM images for EOS-MODIS," *Remote*
794 *Sens. Environ.*, vol. 59, pp. 440–451, 1997.
- 795 [54] W. Wu, "The generalized difference vegetation index (GDVI) for dryland
796 characterization," *Remote Sens.*, vol. 6, pp. 1211–1233, 2014.
- 797 [55] W. Wu et al., "Salinity modeling by remote sensing in central and south-
798 ern Iraq," presented at *Fall Meeting, AGU*, San Francisco, CA, USA,
799 Dec. 3–7, 2012, Abstract B53H-07 [Online]. Available: [http://abstract
800 search.agu.org/meetings/2012/FM/sections/B/sessions/B53H/abstracts/
801 B53H-07.html](http://abstract)
- 802 [56] M. A. Hardisky, V. Klemas, and R. M. Smart, "The influences of soil
803 salinity, growth form, and leaf moisture on the spectral reflectance of
804 *Spartina alterniflora* canopies," *Photogramm. Eng. Remote Sens.*, vol. 49,
805 pp. 77–83, 1983.
- 806 [57] N. H. Abu-Hamdeh and R. C. Reeder, "Soil thermal conductivity effects
807 of density, moisture, salt concentration, and organic matter," *Soil Sci. Soc.*
808 *Amer. J. (SSSAJ)*, vol. 64, pp. 1285–1290, 2000.
- 809 [58] A. R. Sepaskhah and L. Boersma, "Thermal conductivity of soils as
810 a function of temperature and water content," *Soil Sci. Soc. Amer. J.*
811 *(SSSAJ)*, vol. 43, no. 3, pp. 439–444, 1979.



Weicheng Wu received the B.Eng. and M. Eng. 812
degrees in earth sciences from the East China 813
Geological Institute, Fuzhou, Jiangxi, China, in 1986 814
and 1995, respectively, DESS (eq. to M. Eng.) degree 815
in environmental engineering from the University of 816
Paris XI (Paris-Sud), Orsay, France, in 1998, and 817
the Ph.D. degree in geography with specialization in 818
environmental geomatics (including remote sensing, 819
GIS, and spatial analysis) from the University of Paris 820
I (Panthéon-Sorbonne), Paris, France, in 2003. 821

In addition to his 11 years of university teaching 822
and research experience in China, he has gained 16 years of international experi- 823
ence in monitoring environmental changes and problems assessment, and land 824
resources investigation by remote sensing and GIS in Europe (France, Belgium, 825
and Italy) and in the Middle East. From 2005 to 2007, he was a Remote Sensing 826
Expert at NRD, University of Sassari, Sassari, Italy, and from 2007 to 2014, 827
Remote Sensing Specialist with ICARDA (International Center for Agricultural 828
Research in the Dry Areas), Amman, Jordan. He is currently an independent 829
scientist in Choisy-Le-Roi 94600, France. 830

He has played an active role, and partly coordinated and led in 24 national 831
and international cooperation research projects in China, France, Belgium, 832
and Italy and at ICARDA. He has published in total 63 scientific and techni- 833
cal papers, of which 32 are peer-reviewed and 31 are nonpeer-reviewed 834
conference/symposium papers. He serves as Reviewer for more than 12 ISI- 835
refereed and nonrefereed journals in remote sensing and geography. 836

His research interests include land characterization such as land use/cover 837
mapping, multitemporal and time-series change tracking, biomass and carbon 838
sequestration/emission analysis, land degradation assessment, water resources 839
accounting, crop production estimation, human–environmental interaction, and 840
impacts of climate change on water resources and food security. 841

842
843
844
845
846
847
848
849
850
851
852
853
854
855
856
857
858
859

Waleed M. Al-Shafie was born in Baghdad, Iraq, in 1970. He received the B.S. and M.S. degrees in agricultural science, soil, and water resources from the University of Baghdad, Iraq, in 1994 and 2010, respectively.

From 2000 to 2003, he was an Assistant Researcher with IPA Agricultural Research Center, Department of Soil and Water, and from 2003 to 2007, Head of GIS Section, Ministry of Agriculture, Baghdad, Iraq. Since 2010, he has been in charge of the Manage—Planning and Follow-up Office of

the AgroEcological Zoning (AEZ) Department, Ministry of Agriculture in Baghdad, and responsible for the implementation of land suitability maps for main crops in Iraq, while contributing to the development of the AEZ database which includes information of climate, soils, agricultural crops, and socio-economic parameters for Iraq. His research interests include application of geographic information systems (GIS) and remote sensing for AEZ mapping, land suitability analysis, and salinity quantification.

860
861
862
863
864
865
866
867
868
869
870
871
872
873

Ahmad S. Mhaimed received the B.S. degree in soil science from Baghdad University, the M.S. degree in soil survey and classification from the University of Nebraska–Lincoln, Lincoln, NE, USA, and the Ph.D. degree in soil survey from Colorado State University, Fort Collins, CO, USA.

Of 30 years of academic experience, he is currently a Full-time Professor in Soil Survey and Land Management, and Head of the Desertification Control Department, College of Agriculture, Baghdad University, Baghdad, Iraq. He has presented

many papers in national and international conferences and has published 3 books and more than 70 scientific papers. His research interests include soil survey and management using GIS and remote sensing.

874
875
876
877
878
879
880
881
882
883
884
885
886
887
888
889
890
891

Feras Ziadat received the M.Sc. degree in soil conservation from the University of Jordan, and the Ph.D. degree in application of GIS and remote sensing for land use planning in arid areas from Cranfield University, U.K.

After his Ph.D., he worked with the University of Jordan as Associate Professor in Land Resource Management, GIS and remote sensing for 8 years. He currently works as a Soil Conservation and Land Management Specialist with the Integrated Water and Land Management Program, ICARDA. He has pub-

lished over 44 refereed journal and conference proceedings in the area of land and water resources management. His research interests include sustainable land resource management and environmental modeling and monitoring with emphasis on the application of GIS and remote sensing on soil-landscape modeling and digital soil mapping, integrated and participatory land use planning and land evaluation, land degradation and desertification, land use changes, and integrated watershed management.



Vinay Nangia received the Ph.D. degree in water resources science and two M.S. degrees, one in biosystems and agricultural engineering and the other in geographic information science, all from University of Minnesota, Minneapolis, MN, USA.

He is an Agricultural Hydrologist with the International Center for Agricultural Research in the Dry Areas (ICARDA), Amman, Jordan. During a 9-year Postdoctoral research career, he has served as a PI of co-PI on research projects worth about 5.75 million, and authored or coauthored 59 technical pub-

lications that include 22 refereed journal articles in national or international journals. He is an internationally recognized authority in hydrologic and water quality modeling and GIS applications in water resources management. He has offered more than 20 trainings (covering a total of 400 participants) on hydrologic modeling in 10 countries. He has served as Research Advisor/Committee Member to M.S. and Ph.D. students and was a Visiting Assistant Professor (2007–2011) with the Institute of Soil and Water Conservation, Chinese Academy of Science, Beijing, China, where he co-advises graduate students. Previously, he was a NSERC Visiting Fellow with Agriculture and Agri-Food Canada conducting research on GHG emissions from sub-surface tile-drained croplands of Eastern Ontario prior to which he was a Postdoctoral Fellow with the International Water and Management Institute (IWMI), where he started his career in 2005.

Dr. Nangia serves on the Editorial Board of professional society journals.



William Bill Payne received the B.A. degree in chemistry from Wabash College, Crawfordsville, IN, USA, in 1981, and the M.S. and Ph.D. degrees in soil science from the Texas A&M University, College Station, TX, USA, in 1988 and 1990, respectively.

He is the recently appointed Dean of the College of Agriculture, Biotechnology and Natural Resources and Director of the Nevada Agricultural Experiment Station, University of Nevada Reno, Reno, NV, USA. From 2012 to 2014, he worked as Director of a \$150 million CRP1.1 research program with ICARDA

(International Center for Agricultural Research for the Dry Areas), Amman, Jordan, aimed at improving food security and livelihoods in the dry areas of the world. Prior to this, he served as a Professor of Crop Physiology with Texas A&M University, College Station, TX, USA, and is a former Research Director of the Norman Borlaug Institute for International Agriculture.

He has published 11 books and book-chapters, 53 refereed journal papers, and more than 100 nonrefereed conference abstracts and proceedings papers.

Dr. Payne has been named Fellow of five international scientific societies and has held numerous leadership roles at the state, national, and international levels.

892
893
894
895
896
897
898
899
900
901
902
903
904
905
906
907
908
909
910
911
912
913
914
915
916917
918
919
920
921
922
923
924
925
926
927
928
929
930
931
932
933
934
935
936
937
938